International Journal of Latest Research in Science and Technology
Volume 3, Issue 3: Page No. 65-69. May-June 2014
https://www.mnkpublication.com/journal/ijlrst/index.php
ISSN (Online):2278-5299

HIGH PERFORMANCE SUPERCAPACITOR ELECTRODE MATERIAL BASED ON FLOWER LIKE MoS_2/REDUCED GRAPHENE OXIDE NANOCOMPOSITE

[1]Manas Mandal, [1]Debasis Ghosh, [2]Swinderjeet Singh Kalra, [1]Chapal Kumar Das
[1]Materials Science Centre, Indian Institute of Technology Kharagpur, Kharagpur, West Bengal, India
[2]Department of Chemistry, DAV College, Kanpur, India

Abstract*– A simple and cost effective hydrothermal method has been done for the synthesis of MoS_2 and MoS_2/rGO nanocomposites. The prepared MoS_2/rGO composite was characterized by XRD, FESEM and TEM which revealed the formation and as well as the morphological scenario of MoS_2/rGO nanocomposite. Pure MoS_2 and MoS_2/rGO nanocomposite show 3D hierarchical flowery architecture where rGO nanosheets were intercalated into the MoS_2 nanosheets. For the electrochemical performance, cyclic voltammetry and galvanostatic charge discharge measurements were carried out. The composite exhibits maximum specific capacitance of 253 F/g at a current density of 1 A/g with good cycling stability.

Keywords – MoS_2, reduced Graphene Oxide, Pseudocapacitance, Supercapacitor.

I. INTRODUCTION

Climate change and the availability of decreasing fossil fuels are the main reason behind the need of searching for a sustainable, renewable energy resource. In a parallel way, the new inventions like electronic gadgets such as smart phones, tablets, digital camera have made our life easier but the energy consumption per person has been increased frequently and it is also aided the reason why the researchers are going for a cheapest energy source. Therefore, the energy storage systems like electrochemical capacitors are needed. Electrochemical capacitors; also called supercapacitors have attracted a great deal of attention in recent years due to their interesting features such as high power density, fast charging/discharging process, long cycle life and small environmental impact, etc. [1].

Nanostructured materials have fascinated great interest in recent years because of their remarkable mechanical, electrical and optical properties. As a unique carbon nanomaterial, graphene has attracted more importance by virtue of its promising applications in supercapacitor electrodes materials because of its excellent conductivity, superior mechanical properties, exceptionally large specific surface area and chemical stability [2-4]. Recently, for electrochemical energy storage application, metal sulfides-based graphene composites such as In_3S_2/graphene [5] CoS_2/graphene [6] and NiS/graphene [7] have been studied.

MoS_2 is a typical family member of transition-metal dichalcogenides. The structure of MoS_2 facilitates itself to act as an excellent functional material. Here the metal Mo layer is stacked by two S layers held together by weak Van der Waals interactions [8]. The electron-electron correlations of Mo atoms would aid in enhancing planar electric transportation properties. The composites of MoS_2 with conductive carbonaceous materials such as graphene/MoS_2 [9], CNTs/MoS_2 [10], or mesoporous carbon/MoS_2 [11] have been highly explored for anode materials of lithium ion batteries (LIBs), hydrogen production and sensing like many other application field [12, 13].

Herein, we demonstrate an environmentally friendly, one pot hydrothermal synthesis of molybdenum sulfide/reduced graphene oxide (MoS_2/rGO) nanocomposite with the use of ammonium heptamolybdate and thiourea as sulphur source. As an electrode material for supercapacitors, MoS_2/rGO nanocomposite exhibits high specific capacitance of 253 F/g at a current density of 1 A/g with good cycling stability.

II. MATERIALS AND METHOD

IIA Materials used

All materials were used prior to the further purification. Ammonium heptamolybdate was purchased from Merck specialities privet Ltd., Mumbai. Thiourea was purchased from RFCL Ltd., New Delhi. Graphite fine powder, orthophosphoric acid (H_3PO_4), sulfuric acid (H_2SO_4) and hydrochloric acid (HCl) were supplied by Loba Chemie Pvt. Ltd. Mumbai (India). Nafion was purchased from Sigma Aldrich, Germany.

IIB Preparation of graphene oxide (GO)

Graphene oxide was prepared from natural graphite fine powder (extra pure) by modified Hummers method [14]. Briefly, a 9:1 mixture of concentrated H_2SO_4/H_3PO_4 (360:40 mL) was taken with 3.0 gm graphite fine powder. Then 18.0 gm $KMnO_4$ was added pinch by pinch to the mixture solution because enormous heat is produced due to exothermic reaction. After stirring for 12 h the mixture solution was

Publication History
Manuscript Received : *19 June 2014*
Manuscript Accepted : *24 June 2014*
Revision Received : *26 June 2014*
Manuscript Published : *30 June 2014*

cooled to room temperature and poured onto ice (400 mL) with 3ml 30% H_2O_2. The solution was stirred for another 4h and centrifuged at 4000 rpm. The solid material was then washed in succession with water, 20% HCl, and ethanol. The solid material was dried for overnight at 60 ˚C temperature.

IIC Synthesis of MoS_2/rGO nanocomposite

The preparation of layered MoS_2 was conducted by a simple hydrothermal method. Briefly, 20 ml 0.1 M ammonium heptamolybdate and 20ml 0.1 M thiourea aqueous solution were taken with 50 mg graphene oxide and mixture solution was ultrasonicated for 30 min. Then the mixture solution was transferred into a stainless steel autoclave and kept in a furnace at 220 °C for 12h. The black precipitate was washed by water and ethanol, and dried at 65 °C for 12h. The pure MoS_2 was prepared by the same procedure without adding GO.

III. MATERIALS CHARACTERIZATION

The as-prepared products were characterized with X-ray diffractometer (XRD, Rigaku diffractometer with a Cu Kα radiation (λ= 1.54056 Å), field emission scanning electron microscopy (FESEM, Carl Zeiss-SUPRATM 40) and transmission electron microscopy (TEM, TECNAI G2-20S-TWIN).

IIIA Electrochemical measurements

For the electrochemical measurements we used a three electrode system, where active materials fabricated on glassy carbon (GC) electrode, Pt electrode and saturated calomel electrode (SCE) were chosen as working, counter and reference electrode, respectively. For preparation of working electrode, 0.1 mg of the sample was taken in 1% nafion solution (10 µl nafion in 1 ml ethanol) and ultrasonicated for 10 min. The prepared solution was cast onto the glassy carbon electrode (diameter-3 mm) and allowed to dry fully under air. The electrochemical tests, cyclic voltammetry (CV) and galvanostatic charge-discharge technique were performed by using Biologic SP-150 instrument in an aqueous Na_2SO_4 electrolyte (1.0 M).

IV. RESULTS AND DISCUSSION

IVA X-ray diffraction analysis

The XRD patterns of the products are shown in Fig. 1. For Graphene Oxide, the characteristic diffraction peak at about 10^o indicating successful oxidation of the graphite and formation of GO [15]. For pure MoS_2, the diffraction peaks are well matched with the JCPDS Card No. 37-1492. The peaks appear at 14.2, 33.5, 39.8, 43.1, 49.1 and 59.3^o corresponding to (002), (100), (103), (006), (105) and (110) planes, respectively. For MoS_2/RGO nanocomposite, all of the characteristic peaks of pure MoS_2 are present there but there is no obvious peak for the GO component. Only the broad peak observed at 2θ = 24–30° indicates the presence of RGO sheets [16].

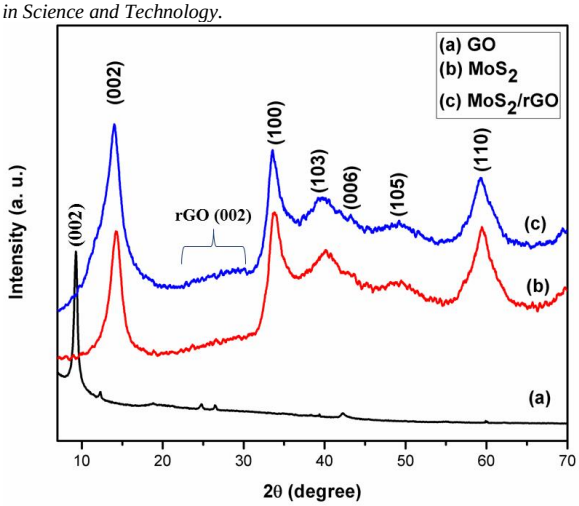

Fig. 1 XRD pattern of the as synthesized (a) GO, (b) MoS_2 and (c) MoS_2/rGO nanocomposite

IVB Morphological analysis

Fig.2 shows the FESEM images of the as prepared MoS_2 and MoS_2/rGO nanocomposite indicating the formation of 3D hierarchical flowery architecture. Each flower consists of several interconnected nanopetals in the form of nanosheets. The average diameter of the flowers are about 180 - 200 nm. In the MoS_2/rGO nanocomposite, the interconnected flowery morphology of the MoS_2 retains with an increased flower diameter. A close inspection of the flowers in the composite reveals its porous architecture where the rGO nanosheets intercalate into the MoS_2 nanosheets. This intercalation is the main reason behind the increased interconnected flower diameter. Porous and flexible rGO with its high conductivity forms an interconnected conducting network and facilitates rapid electronic transport in electrode reactions and also increases the specific surface area of the composite. It is well known that porous nanostructures possess superior charge storage behavior, when compared to that of the bulk structures. Furthermore, this 3D flower-like structure also enhances the stability of the MoS_2/rGO nanocomposite due to superstrength of rGO.

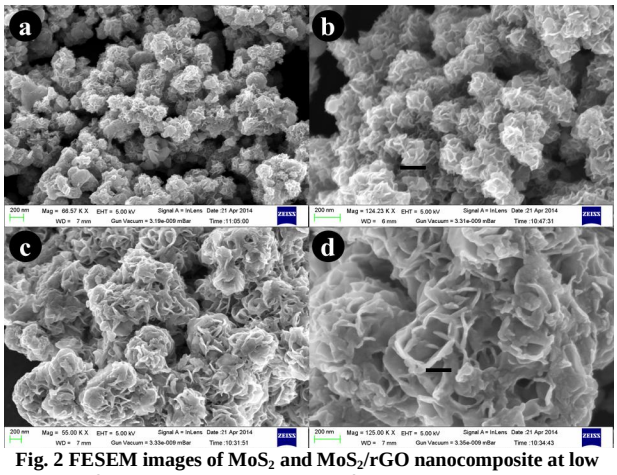

Fig. 2 FESEM images of MoS_2 and MoS_2/rGO nanocomposite at low magnification (a, c), and high magnification (b, d), respectively

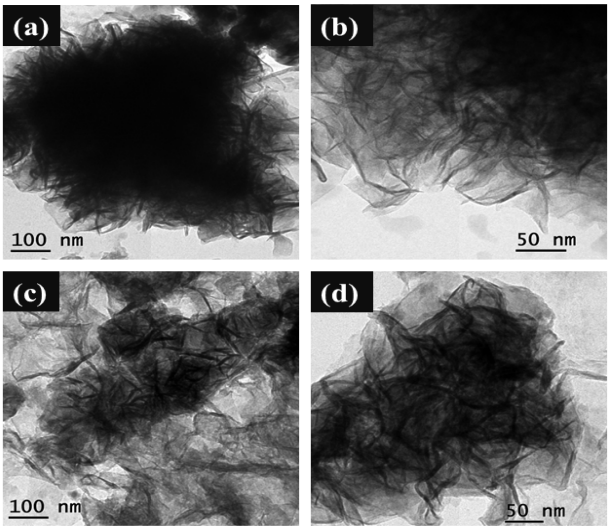

Fig. 3 TEM images of MoS_2 and MoS_2/rGO nanocomposite at low magnification (a, c), and high magnification (b, d), respectively

Fig. 3 shows the TEM images of as synthesized MoS_2 and MoS_2/rGO nanocomposite, supporting the layered nanosheets obtained from FESEM images. The structural and morphological compatibility between rGO and single-layer MoS_2 sheets give a better integration to achieve the anticipated benefits of such integration. This tighter integration between MoS_2 and rGO could synergize their interaction to significantly improve the electrochemical performance of the MoS_2/rGO nanocomposite as materials for supercapacitor.

IVC Electrochemical Study

IVC1 Cyclic voltammetry

The electrochemical properties of the products were studied by cyclic voltammetry (CV) and galvanostatic charge-discharge (GCD) techniques. Fig. 4 shows the cyclic voltammetry analysis at various scan rates in the potential range of (-)0.1 – 0.5 V. From the Fig. 4, it is observed that MoS_2/rGO nanocomposite has largest area surrounded by CV curve, indicating higher specific capacitance and the synergistic effect of MoS_2 and rGO. Additionally, it was found that quasi-rectangular shapes for all CV curves at various scan rates, indicating all materials shows good capacitive behavior. The large area at a high scan rate for a CV curve does not mean a higher capacitance because the effective interaction between the electrolyte ions and the electrode is greatly reduced with the increasing of scan rate. The possible mechanism is based on the pseudo-capacitive behavior due to the faradaic charge transfer process. During the redox process, there occurs intercalation of alkali metal Na^+ in the MoS_2 interlayers upon reduction, followed by deintercalation upon oxidation [17]

$$MoS2 + Na^+ + e- \leftrightarrow MoS–SNa^+$$

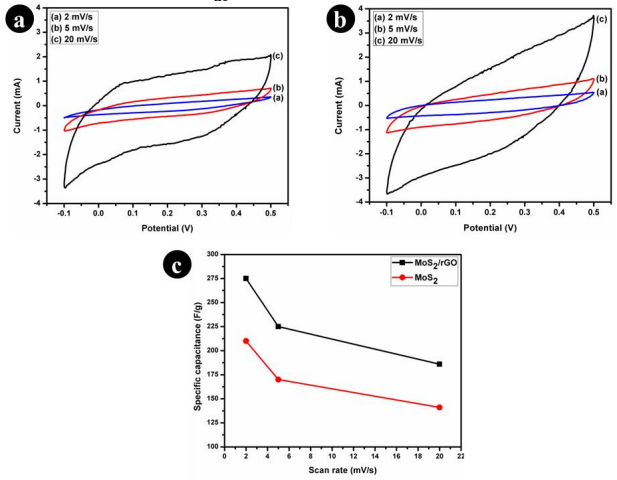

Fig. 4 Cyclic voltammetry curves of MoS_2 (a) and MoS_2/rGO composite (b) at different scan rate of 2, 5 and 20 mV/s. Variation of Specific capacitance as a function of scan rate (c) of MoS_2 and MoS_2/rGO nanocomposite.

The specific capacitance (C_{sp} in F/g) of the composites from the CV measurement can be calculated by using the following equation

$$\text{Specific capacitance } (C_{sp}) = \frac{\int_{V2}^{V1} i(V)dV}{(V2-V1)\nu m}$$

where, i (A) is the instantaneous current in cyclic voltammogram, ν is the potential scan rate (mV/s). V1 and V2 are the switching potential, m is the mass of the electrode and $\int_{V2}^{V1} i(V)dV$ determines the area of the I-V curve. The variations of specific capacitance with scan rate for the pure MoS_2 and MoS_2/rGO nanocomposites are shown in Table 1. From the CV measurements, it is clear that at a scan rate of 2 mV/s, the highest specific capacitance exhibited by MoS_2/rGO composites is 275 F/g, whereas the pure MoS_2 shows a lower specific capacitance of 210 F/g at the same scan rate. Fig. 4(c) is the plot of the specific capacitance of pure MoS_2 and MoS_2/rGO composite as a function of the scan rates based on the CV curves.

TABLE -1 THE VARIATIONS OF SPECIFIC CAPACITANCE WITH SCAN RATE FOR THE PURE MOS_2 AND MOS_2/rGO NANOCOMPOSITES.

Materials	Specific capacitance (F/g) at different scan rate		
	2 mV/s	5 mV/s	20 mV/s
MoS_2	210	170	141
MoS_2/rGO	275	225	186

IVC2 Galvanostatic Charge-discharge measurements

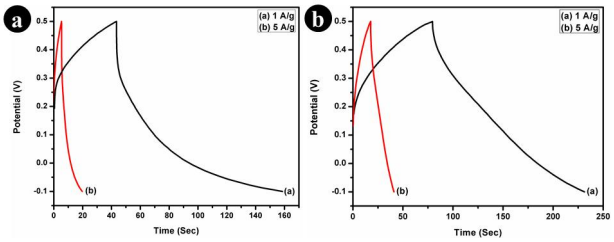

Fig. 5 Galvanostatic charge-discharge curves of MoS_2 (a) and MoS_2/rGO nanocomposites (b) at different current density of 1 and 5 A/g, respectively

Fig. 5 shows the galvanostatic charge-discharge curves of MoS_2 and MoS_2/rGO nanocomposites at different current densities (1 and 5 A/g). The semi-symmetric GCD curves for both the materials reveal their pseudocapacitive behavior. The specific capacitance (C_{sp}) was calculated from the equation below

$$\textbf{Specific capacitance, } C_{sp} = \frac{i \times \Delta t}{m \times \Delta v}$$

where, i, m, Δt and Δv is the applied current (A), mass (g) of the active material, discharge time and potential window, respectively. The variations of specific capacitance with current density for the pure MoS_2 and MoS_2/rGO composites are shown in Table 2.

TABLE -2 THE VARIATIONS OF SPECIFIC CAPACITANCE WITH CURRENT DENSITY FOR THE PURE MOS_2 AND MOS_2/rGO NANOCOMPOSITES

Materials	Specific capacitance (F/g) at different current density	
	1 A/g	5 A/g
MoS_2	194	119
MoS_2/rGO	253	192

Fig. 6(a) shows the variation of the specific capacitance (F/g) with the current density (A/g) of MoS_2 and MoS_2/rGO nanocomposites. The specific capacitances of the MoS_2/rGO electrode at 1 and 5 A/g are 253 F/g and 192 F/g, respectively. The results indicate that the MoS_2/rGO composites have high specific capacitance value as one of the most important electrochemical properties for the electrode materials in the supercapacitor application field.

The advantages of MoS_2/rGO composites electrode over the MoS_2 electrodes are mainly intercalation of rGO nanosheets into the 3D flowery MoS_2 which improves the diffusion rate of ions within the bulk of the materials and also rGO behaves as a highly conductive current collector as its conjugative structure. This is why MoS_2/rGO composite shows better electrochemical performance.

Energy density and power density of the materials were calculated by the following equations

$$\text{Energy density (E)} = \frac{1}{2} C_{sp}(\Delta V)^2$$

$$\text{Power density (P)} = \frac{E}{T}$$

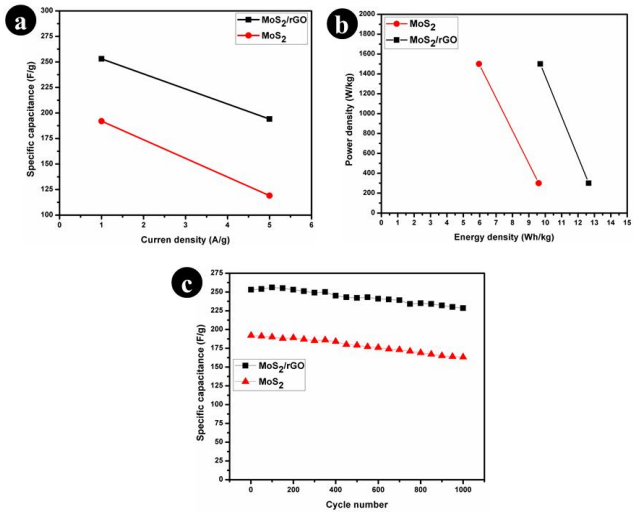

Fig. 6 Variation of Specific capacitance as a function of (a) current density and (c) cycle number of MoS_2 and MoS_2/rGO composites. (b) Ragone plot of MoS_2 (a) and MoS_2/rGO composite.

where, C_{sp} = specific capacitance in F/g, and ΔV = potential window in volt, T is the discharge time of the charge-discharge curves from where the specific capacitance was calculated. The variation of energy density and power density with the current densities for both the materials are shown in Table 3.

TABLE -3 CALCULATED POWER DENSITY (W/kg) AND ENERGY DENSITY (Wh/kg) FROM CHARGE-DISCHARGE MEASUREMENT

Electrode Materials	Power density (W/kg) at different current density (A/g)		Energy density (Wh/kg) at different current density (A/g)	
	1 A/g	5 A/g	1 A/g	5 A/g
MoS_2	300	1500	9.6	5.96
MoS_2/rGO	300	1500	12.65	9.7

Fig. 6(b) shows the energy density versus power density curve in terms of Ragone plot. It can be seen from the Ragone plot, as the power density increases from 300 W/kg to 1500 W/kg, the energy density of MoS_2 decreases from 9.6 Wh/kg to 3.2 Wh/kg and the energy density of MoS2/rGO nanocomposite decreases from 12.65 Wh/kg to 9.7 Wh/kg, respectively.

The cycle stability of MoS_2 and MoS_2/rGO nanocomposites were evaluated by repeating the constant current charge-discharge test between (-)0.1 and 0.5 V (vs. SCE) at a current density of 1.0 A/g for 1000 cycles. The retention of specific capacitance of MoS_2 and MoS_2/rGO nanocomposites are 85% and 90.3% of the initial capacitance, respectively. From the Fig. 6(c), apart from the initial increase of specific capacitance upto 100 cycles a linear decay can be seen. The initial increase is a consequence of wetting effect.

V. CONCLUSIONS

Layered MoS_2 and MoS_2/rGO nanocomposite with 3D hierarchical flowery architecture were synthesized by a

simple and cost effective one pot hydrothermal process. The maximum specific capacitance for MoS_2/rGO is 253 F/g at a current density 1 A/g compared to 194 F/g for MoS_2. The integration of graphene into the composites provides relatively large areas to loading MoS_2 sheets, leading to three-dimensional nanostructures. Thus MoS_2/rGO composites enable an easy access for both charge-transfer and ion transport throughout the electrode. Furthermore, the capacitance retention is still over 90.3% of initial capacitance after 1000 cycles. These results suggest that the MoS_2/rGO nanocomposites are quite a suitable and promising electrode material for high-performance supercapacitor.

ACKNOWLEDGMENT

The authors thank Indian Institute of Technology Kharagpur, India for financial support and instrumental help.

REFERENCES

[1] Conway B.E. "Electrochemical Supercapacitors, Scientific Fundamental and Technological Applications" Kluwer Academic/Plenum Publishers, New York, 1999.

[2] Zhu Y.W., Murali S., Stoller M.D., Ganesh K.J., Cai W.W., Ferreira P.J., Pirkle A., Wallace R.M., Cychosz K.A., Thommes M. "Carbon-based supercapacitors produced by activation of graphene" Science, Vol. 332, No. 6037, pp. 1537-1541, 2011.

[3] Sun Y.Q., Wu Q., Shi G.Q. "Graphene based new energy materials" Energy & Environmental Science, Vol. 4, pp. 1113-1132, 2011.

[4] Zhai Y., Dou Y., Zhao D., Fulvio P.F., Mayes R.T., Dai S. "Carbon Materials for Chemical Capacitive Energy Storage" Advanced Materials, Vol. 23, Issue 42, pp. 4828–4850, 2011.

[5] Ye F., Du G., Jiang Z., Zhong Y., Wang X., Cao Q., Jiang J.Z. "Facile and rapid synthesis of RGO–In_2S_3 composites with enhanced cyclability and high capacity for lithium storage" Nanoscale, Vol. 4, pp. 7354-7357, 2012.

[6] Qu B., Chen Y., Zhang M., Hua L., Lei D., Lu B., Li Q., Wang Y., Chen L., Wang T. "β-Cobalt sulfide nanoparticles decorated graphene composite electrodes for high capacity and power supercapacitors" Nanoscale, Vol. 4, pp. 7810-7816, 2012.

[7] Pan Q., Xie J., Liu S., Cao G., Zhu T., Zhao X. "Facile one-pot synthesis of ultrathin NiS nanosheets anchored on graphene and the improved electrochemical Li-storage properties" RSC Advances, Vol. 3, pp. 3899-3906, 2013.

[8] Ma G., Peng H., Mu J., Huang H., Zhou X., Lei Z. "In situ intercalative polymerization of pyrrole in graphene analogue of MoS_2 as advanced electrode material in supercapacitor" Journal of Power Sources, Vol. 229, pp. 72-78, 2013.

[9] Chang K., Chen W. "In situ synthesis of MoS_2/graphene nanosheet composites with extraordinarily high electrochemical performance for lithium ion batteries" Chemical Communications, Vol. 47, pp. 4252-4254, 2011.

[10] Ding S., Chen J.S., Lou X.W. "Glucose-Assisted Growth of MoS_2 Nanosheets on CNT Backbone for Improved Lithium Storage Properties" Chemistry - A European Journal, Vol. 17, pp. 13142–13145, 2011.

[11] Zhou X., Wan L.J., Guo Y.G. "Facile synthesis of MoS2@CMK-3 nanocomposite as an improved anode material for lithium-ion batteries" Nanoscale, Vol. 4, pp. 5868-5871, 2012.

[12] Zhou W., Yin Z., Du Y., Huang X., Zeng Z., Fan Z., Liu H., Wang J., Zhang H. "Synthesis of few-layer MoS_2 nanosheet-coated TiO_2 nanobelt heterostructures for enhanced photocatalytic activities" Small, Vol. 9, pp. 140–147, 2013.

[13] Huang X., Zeng Z., Zhang H. "Metal dichalcogenide nanosheets: preparation, properties and applications" Chemical Society Reviews, Vol. 42, pp. 1934-1946, 2013.

[14] Marcano D.C., Kosynkin D.V., Berlin J.M., Sinitskii A., Sun Z., Slesarev A., Alemany L.B., Lu W., Tour J.M. "Improved Synthesis of Graphene Oxide" *ACS Nano*, Vol. 4(8), pp 4806–4814, 2010.

[15] Ding S., Chen J.S., Luan D., Boey F.Y.C., Madhavi S., Lou X.W. "Graphene-supported anatase TiO_2 nanosheets for fast lithium storage" Chemical Communication, Vol. 47, pp. 5780-5782, 2011.

[16] Tian J., Li H., Xing Z., Wang L., Luo Y., Asiri A.M., Al-Youbi A.O., Sun X. "One-pot green hydrothermal synthesis of CuO–Cu_2O–Cu nanorod-decorated reduced graphene oxide composites and their application in photocurrent generation" Catalysis Science & Technology, Vol. 2, pp. 2227-2230, 2012.

[17] Soon J.M., Loh K.P. "Electrochemical Double-Layer Capacitance of MoS_2 Nanowall Films" Electrochemical and Solid-State Letters, Vol. 10, pp. A250-A254, 2007.